



UNIVERSITY OF THE PHILIPPINES

Bachelor of Science in Applied Physics

Clarence Ioakim T. Sy

*Classroom learning dynamics using a cellular automata spatiotemporal model comparing peer instruction and traditional instruction*

Thesis Adviser:

Johnrob Y. Bantang, Ph.D.

National Institute of Physics

University of the Philippines Diliman

Date of Submission:

July 2025

Thesis Classification:

F

*This thesis is available to the public*

National Institute of Physics  
College of Science  
University of the Philippines  
Diliman, Quezon City

## **ENDORSEMENT**

This is to certify that this thesis entitled **Classroom learning dynamics using a cellular automata spatiotemporal model comparing peer instruction and traditional instruction**, prepared and submitted by Clarence Loakim T. Sy in partial fulfillment of the requirements for the degree of Bachelor of Science in Applied Physics, is hereby accepted.

JOHNROB Y. BANTANG, Ph.D.  
Thesis Adviser

The National Institute of Physics endorses acceptance of this thesis in partial fulfillment of the requirements for the degree of Bachelor of Science in Applied Physics.

WILSON O. GARCIA, Ph.D.  
Director  
National Institute of Physics

To thinking complexly

# Acknowledgments

I would like to thank...

**My family**, for making sure I don't have to think about more things than I have to throughout my learning years, even in college. Thank you also for always providing more than what I need, and sometimes even more than what I want. I couldn't have afforded to be so carefree without you.

**Dr. Johnrob Bantang**, my adviser, for your patience, understanding, and guidance, for often treating us with food, and for the corniest and nerdiest jokes. Thank you for making a CSG a place for nerds to be nerds, and for making all kinds of ideas welcome.

**The Complexity Science Group**. Reinier: for always being someone we can rely on and relate with. Laya and Sara: for making sure I felt at home with the group, especially when I first joined. Jer: for all the times we were lost together, both in class and in research, but figured things out one way or another. Philip, Rwen, and Renzo: for all the talks and laughs about so many random things from physics to toilets to running.

**The Flahtotoys**, who are always there to support me with whatever problems I have, to share in my nerdy enthusiasm, and to go on so many adventures with. Thanks for the Manila totoys, Hanzel, Jerahmeel, and Atty. Carl, for all the times we go jogging, hiking, and eating Rodics. To the moms, especially to Pong and Sel, thanks for always looking out for me and being there to listen. Char, thanks for being someone I can always talk to and rely on for scout and photography matters.

**Julia**, for believing in me and for appreciating me simply for who I am, flaws and all. Thank you for doing your very best to always be there for me, for always being patient and understanding with me, and for always being proud of me no matter what mistake I make.

**Janella**, for always matching my energy when I talk about literally anything, and for being someone I can confide in without fear of judgement.

**Ms. Danielle**, for helping me learn how to be kind to myself and for always being there to listen to me, even when I'm not sure what I'm saying. The things I tell myself when I'm in doubt are mostly things that came from you. Thank you for being that voice in my head that helps me be kind to myself.

**The Hexagon**, Matt and Darwin, for being the constants that you are since we met and for being people I can talk to about my problem(set)s, with topics ranging from electrodynamics and quantum mechanics to where we'll be eating lunch. You have helped me stay sane and have been constant reminders that there's much joy in being nerds together, even if what we end up talking about isn't remotely nerdy.

**The Stephenian Scout Group**, for always welcoming me back to a place where I can do what I enjoy outside the academe. Marc: for being someone I can turn to for knowledge and wisdom about the so many interests we share. Sid, Francynne, Chester, Kim, and Sam: for always being supportive and being g for the most random galas.

**The Cakes**, for being people I can talk about the latest meta and math for our favorite gacha games, and for sharing the struggles of being college students even if we're all in different schools.

**The 401 tambays**, Belle, Eli, Edneil, and Mika, for always being there to keep me company when I don't feel like going home for the day yet, and for inviting me to your occasional lakwatsas.

**Monica**, for being unfathomably patient and supportive when I needed someone to be just that.

I can't list them all, but none of what any of you have done goes unappreciated. From the bottom of my heart, thank you.

## ABSTRACT

### CLASSROOM LEARNING DYNAMICS USING A CELLULAR AUTOMATA SPATIOTEMPORAL MODEL COMPARING PEER INSTRUCTION AND TRADITIONAL INSTRUCTION

Clarence Ioakim T. Sy  
University of the Philippines (2025)

Adviser:  
Johnrob Y. Bantang, Ph.D.

Peer instruction has recently become one of the popular means of classroom instruction in Physics Education. Such educational setup must involve both physical interaction with things and actually doing some procedural steps mentally or physically. In this study, we investigate the effects of different seating arrangements on the students' learning efficiency in peer instruction by modeling the transfer of knowledge within the class as a probabilistic cellular automata model. We compared the efficiency of learning between the traditional learning model and the peer instruction model. We found that in square classrooms with different lengths  $L \in \{32, 48, 64, 96, 128\}$ , the inner corner seating arrangement performed the best among the peer instructions setups in terms of both the time  $t_{max}$  it takes for all the students to learn and the classroom's learning rate  $m$ . This result is different from a previous study, where they found that the outer corner seating arrangement performed the best. The difference stems from the simplifications made in this model that may not reflect real world factors. Our model uses binary values in an isotropic system and does not consider memory or unlearning. However, despite these simplifications, we found that in smaller classrooms with slow learners, peer instruction is more efficient compared to the traditional learning model, just as previous studies have suggested.

Taken from SPP-2024 paper

PACS: 01.20.+x [Communication forms and techniques (written, oral, electronic, etc.)], 01.30mm (Textbooks for graduates and researchers)

# Table of Contents

<b>Acknowledgments</b>	iii
<b>Abstract</b>	v
<b>List of Figures</b>	vii
<b>1 Peer Instruction and Traditional Models of Teaching</b>	<b>1</b>
1.1 History of Peer Instruction . . . . .	1
1.2 Difference of Peer Instruction from Traditional Models . . . . .	2
1.2.1 Details of Peer Instruction . . . . .	2
1.2.2 Benefits of Peer Instruction . . . . .	2
1.2.3 Drawbacks of Peer Instruction . . . . .	2
1.2.4 Existing models of Peer Instruction . . . . .	2
1.3 Problem statement . . . . .	2
<b>2 The Classroom as a PCA</b>	<b>3</b>
2.1 Cellular Automata and its use in modelling complex systems . . . . .	3
2.2 PCA model for classroom dynamics . . . . .	5
2.2.1 Traditional . . . . .	5
2.2.2 Peer instruction (PI) . . . . .	6
2.3 Results: Homogenous PI vs Traditional . . . . .	10
2.3.1 Time to learn $t_{max}$ vs positional learning factor $\rho_0$ . . . . .	10
2.3.2 Class learning rate $m$ vs positional learning factor $\rho_0$ . . . . .	12
2.3.3 Time to learn $t_{max}$ vs class size $N$ . . . . .	14
2.4 Discussion/conclusions? . . . . .	15
<b>3 Heterogeneous Learning Rates</b>	<b>17</b>
3.1 Effects on classroom evolution . . . . .	17
3.1.1 Peer Instruction Models . . . . .	17
3.1.2 Traditional Models . . . . .	18
3.1.3 Comparing temporal learning dynamics of different classroom configurations . . . . .	18
3.2 Class learning rate $m$ vs positional learning factor $\rho_0$ . . . . .	24
3.3 Time to learn $t_{max}$ vs positional learning factor $\rho_0$ . . . . .	26
3.4 Class learning rate $m$ vs heterogeneity $\delta\lambda$ . . . . .	29
3.5 Time to learn $t_{max}$ vs heterogeneity $\delta\lambda$ . . . . .	29
3.6 Discussions/Conclusions? . . . . .	29

<b>4 Mixed Model Instuction</b>	<b>31</b>
4.1 Equations and sub-equations . . . . .	31
<b>5 Conclusions</b>	<b>32</b>
<b>A Sample appendix</b>	<b>33</b>
A.1 Derivation of Equation 2.3 . . . . .	33
A.2 Equations in appendix . . . . .	34
A.3 Codes as appendix . . . . .	34

# List of Figures

2.1	Traditional instruction flowchart . . . . .	6
2.2	Peer instruction flowchart . . . . .	7
2.3	Peer instruction seating arrangements. . . . .	8
2.4	Sample classroom evolution for $L = 64$ , $\lambda_0 = 1$ , and $\rho_0 = 0.5$ with the inner corner SA. Black squares represent learned students while white squares represent unlearned students. The accompanying graphs show the fraction of learned students as a function of time. The blue circle represents the data points while the orange line shows the power law fit. The broken pink line shows the where we truncate the data for fitting the power law and the green line shows the current time step in the plot. . . . .	9
2.5	Time to learn $t_{max}$ as a function of positional learning factor $\rho_0$ for different classroom sizes $L \in \{32, 48, 64, 96, 128\}$ . Lower time to learn $t_{max}$ indicate better performance. . . . .	11
2.6	Class learning rate $m$ as a function of positional learning factor $\rho_0$ for different classroom sizes $L \in \{32, 48, 64, 96, 128\}$ . Higher class learning rate $m$ values indicate better performance. . . . .	13
2.7	Class size dependence of time to learn in homogenous models . . . . .	14
2.8	Distance $d_{max}$ of any student to a high aptitude or learned student for different seating arrangements. . . . .	16
3.1	Sample classroom evolutions for the inner corner SA with $L = 128$ at different times $t$ for positional learning rate $\rho_0 = 0.1$ , $\delta\lambda = 0.4$ . Dark blue squares represent learned students with learning rate $\lambda = \lambda_0 + \delta\lambda$ , blue squares represent learned students with learning rate $\lambda = \lambda_0 - \delta\lambda$ , and light squares represent unlearned students. The accompanying graph shows the fraction of learned students as a function time step. The blue dots represent data points. The yellow line shows the power law fit. The pink dashed vertical line shows where we truncate the data for fitting the power law. The green vertical line shows the current time step in the simulation. . . . .	19

3.2	Sample classroom evolutions for the inner corner SA with $L = 128$ at different times $t$ for positional learning rate $\rho_0 = 0.9$ , $\delta\lambda = 0.1$ . Dark blue squares represent learned students with learning rate $\lambda = \lambda_0 + \delta\lambda$ , blue squares represent learned students with learning rate $\lambda = \lambda_0 - \delta\lambda$ , and light squares represent unlearned students. The accompanying graph shows the fraction of learned students as a function time step. The blue dots represent data points. The yellow line shows the power law fit. The pink dashed vertical line shows where we truncate the data for fitting the power law. The green vertical line shows the current time step in the simulation. . . . .	20
3.3	Sample classroom evolutions for the inner corner SA with $L = 128$ at different times $t$ for positional learning rate $\rho_0 = 0.9$ , $\delta\lambda = 0.4$ . Dark blue squares represent learned students with learning rate $\lambda = \lambda_0 + \delta\lambda$ , blue squares represent learned students with learning rate $\lambda = \lambda_0 - \delta\lambda$ , and light squares represent unlearned students. The accompanying graph shows the fraction of learned students as a function time step. The blue dots represent data points. The yellow line shows the power law fit. The pink dashed vertical line shows where we truncate the data for fitting the power law. The green vertical line shows the current time step in the simulation. . . . .	21
3.4	Sample classroom evolutions for the inner corner SA with $L = 128$ at different times $t$ for positional learning rate $\rho_0 = 0.9$ , $\delta\lambda = 0.4$ . Dark blue squares represent learned students with learning rate $\lambda = \lambda_0 + \delta\lambda$ , blue squares represent learned students with learning rate $\lambda = \lambda_0 - \delta\lambda$ , and light squares represent unlearned students. The accompanying graph shows the fraction of learned students as a function time step. The blue dots represent data points. The yellow line shows the power law fit. The pink dashed vertical line shows where we truncate the data for fitting the power law. The green vertical line shows the current time step in the simulation. . . . .	22
3.5	Comparison of time to learn $t_{max}$ and fraction of learned students for different representative classroom configurations. Each SA corresponds to a different color, blue for traditional, yellow for inner corner, green for outer corner, orange for center, and pink for random. Different values $\rho_0$ corresponds to varying alpha or transparency, where lower $\rho_0$ values are more transparent. Different values of $\delta\lambda$ corresponds to different line styles, where $\delta\lambda = 0.0$ are represented by dashed lines, $\delta\lambda = 0.2$ are represented by lines with alternating dots and dashes, $\delta\lambda = 0.4$ are represented by two dots followed by a dash. Different classroom sizes $L$ corresponds to different line widths, where bigger classroom sizes correspond to thicker lines. The bands around each line show the standard deviation of the data over 5 trials. Higher fraction of learned indicates better performance. . . . .	23

- 3.6 Representative plots for class learning rate  $m$  as a function of positional learning coefficient  $\rho_0$ . Each subplot represent a different SA and classroom size  $L$ . In each plot, the circles represent the data points, color represents a different value of  $\delta\lambda \in \{0.0, 0.1, 0.2, 0.3, 0.4\}$ , dashed lines connect the data points for  $\delta\lambda \in \{0.0, 0.4\}$ . Higher class learning rate  $m$  values indicate better performance. . . . . 25
- 3.7 Time to learn  $t_{max}$  as a function of positional learning factor  $\rho_0$  for different representative classroom configurations and sizes with varying heterogeneity  $\delta\lambda \in \{0, 0.1, 0.2, 0.3, 0.4\}$ . Lower time to learn  $t_{max}$  indicates better performance. . . . . 27
- 3.8 Time to learn  $t_{max}$  as a function of positional learning factor  $\rho_0$  for the heterogeneous model of all seating arrangements and classroom sizes  $L$ . Each ribbon series represent the range of values for  $t_{max}$  for a given seating arrangements with heterogeneity  $\delta\lambda = \{0.0, 0.1, 0.2, 0.3, 0.4\}$ . Lower time to learn  $t_{max}$  indicates better performance. . . . . 28
- 3.9 Time to learn  $t_{max}$  as a function of heterogeneity  $\delta\lambda$  for the heterogeneous models of the PI (inner corner SA) and traditional models with varying positional learning factor  $\rho_0 \in \{0.3, 0.5, 0.7\}$  and classroom sizes  $L \in \{32, 128\}$ . Each color represents a diffent value of  $\rho_0$ , while the circle and square symbols represent the traditional and PI models respectively. Lower time to learn  $t_{max}$  indicates better performance. . . . . 29

# Chapter 1

## Peer Instruction and Traditional Models of Teaching

something

### 1.1 History of Peer Instruction

Something something Mazur something something

## **1.2 Difference of Peer Instruction from Traditional Models**

- 1.2.1 Details of Peer Instruction**
- 1.2.2 Benefits of Peer Instruction**
- 1.2.3 Drawbacks of Peer Instruction**
- 1.2.4 Existing models of Peer Instruction**

- Nitta mathematical models of PI [4]
- roxas2010seating [5]

## **1.3 Problem statement**

point is to propose an alternate model for a dynamical something

# Chapter 2

## The Classroom as a PCA

The classroom is a complex system that can be modeled as a probabilistic cellular automata (PCA). This chapter will discuss the classroom as a complex system and the probabilistic cellular automata model. The chapter will also discuss the implications of the model on the classroom and the teaching-learning process. (AI Generated Text)

Probably add objectives here???

### 2.1 Cellular Automata and its use in modelling complex systems

A two-dimensional (2D) rectangular cellular automata can be defined by a five-tuple [1] + Reinier MS:

$$\text{CA} = \{\mathcal{S}, \mathcal{C}, \mathcal{L}, \mathcal{N}, \mathcal{R}\} \quad (2.1)$$

where

$\mathcal{S}$  = is the set of possible states that each cell can assume. The state  $s$  can use any kind of representation such as the set of integers  $\{0, \dots, n - 1\}$  with  $n$  as the total number of possible states.

$\mathcal{C} = \{c = i, j \mid i \in \{1, 2, 3, \dots, L_1\}, j \in \{1, 2, 3, \dots, L_2\} \text{ s.t. } L_1 \times L_2 = N\}$  is the set of identifiers for each cell in the automaton where  $N$  is the total number of cells and  $L_1$  and  $L_2$  are the lengths of each side of the automaton space. The cells can then be identified by their position in the automaton  $(i, j)$ . So, the state of cell  $c \in \mathcal{C}$  can be written as  $s_c = s_{i,j} \in \mathcal{S}$

$\mathcal{L} =$  defines the lattice neighborhood which is generally a mapping  $f : \mathcal{C} \rightarrow C^M$  where  $M$  is the number of neighbors of a cell  $c \in \mathcal{C}$ . Any given cell  $c$  is mapped to another tuple of cells:  $L_{i,j} = \{(i-1, j-1), (i-1, j), (i-1, j+1), (i, j-1), \dots, (i, j)\}$ . Where  $r$  is the radius of the Moore neighborhood. We then say that  $\mathcal{L}_{i,j}$  contains the set of neighboring cell for  $c_{i,j}$ .

$\mathcal{N} = \mathcal{S}^M$ , the set of neighborhood states. Thus,  $N_c = N_{i,j} \in \mathcal{N}$  such that each  $\mathcal{N}$  is in the form of the  $M$ -tuple  $\{s_{i-1,j-1}, s_{i-1,j}, s_{i-1,j+1}, s_{i,j-1}, \dots, s_{i,j}\}$ .

$\mathcal{R} =$  defines the set of rules implemented in the CA with  $g : s_{i,j} \mid \mathcal{L} \rightarrow \mathcal{S}$  as the mapping of any neighborhood state  $N_c$  to a new state  $s'_{i,j}$  of the cell  $c$ . At the next time step,  $s'_{i,j}$  replaces the original state  $s_{i,j}$ .

$\mathcal{N}$  can vary with the neighborhood structure and the boundary conditions of the automaton. The neighborhood structure dictates the shape the neighborhood in the lattice. Common neighborhood structures include the von Neumann (diamond) and Moore (square) neighborhoods. Boundary conditions dictate how the automaton treats cells at the egde of the lattice when determining the neighborhood. Common boundary conditions include toroidal, spherical, and fixed boundary conditions.

$\mathcal{R}$  can also be affected by other factors such as whether the rules are deterministic or probabilistic and whether they are implemented synchronously or asynchronously. An automaton with deterministic rules will always produce the same output given the same input, while an automaton with probabilistic rules will produce different outputs given the same input. In Conway's Game of Life, a cell dies when it has three live neighbors, while a cell is born when it has two or three live neighbors. This is an example of a deterministic rule. An example of a probabilistic rule would be a cell dying with a probability of 0.25 when it has three live neighbors. An automaton with synchronous rules will update all cells simultaneously, while an automaton with asynchronous rules will update cells one at a time. (something explanation something about sync vs async)

Due to the flexibility of cellular automata, they can be used to model a wide variety of complex systems. Cellular automata have been used to model physical systems such as fluid dynamics, biological systems such as the spread of diseases, and social systems such as traffic flow [3]. Its discreteness and locality make it a good model for systems that are composed of many interacting parts. Thus, we have chosen

to use a two-state probability cellular automata to simulate the learning process for students in the classroom

## 2.2 PCA model for classroom dynamics

We used a two-dimensional binary probabilistic cellular automata (PCA) model to simulate the learning process in a classroom. In this PCA model, each cell in the automaton represents a student and the state of each cell represents their aptitude  $S = \{\text{unlearned, learned}\} = \{0, 1\}$ . We assign the neighborhood to be an outer-totalistic Moore neighborhood of radius  $r = 1$  and define the boundary conditions to be fixed wherein the grid does not wrap around itself and  $s_{i,j} = 0$  for  $i, j \notin [1, L]$ . How the automaton updates varies on the learning set up of the classroom. In this study we tackle two learning set ups: traditional and peer instruction (PI). We take the traditional instruction to be the case where the teacher is the only source of information for the students - which is typical for classes where the time is mostly spent on lectures. In the PI set up, we consider that the students learn from each other but only when the students of interest already know the lesson or is in the learned state.

### 2.2.1 Traditional

To model the learning process in the traditional classroom, we set the probability for the student to learn in each time  $P_{ij}$  to be dependent only on their individual learning rates  $\lambda_{i,j}$ , which describes how receptive they are to learning, and the probability for the student to learn from the teacher  $\rho_0$ .

$$P_{ij} = \lambda_{ij}\rho_0 \quad (2.2)$$

where

$P_{i,j} \in [0, 1]$  is the probability of student  $c_{i,j}$  to learn in each time step,

$\lambda_{i,j} = 1$  is the learning rate of student  $c_{i,j}$

$\rho_0 \in [0, 1]$  is the probability of  $c_{i,j}$  to learn from the teacher

In five-tuple form, the traditional PCA model for the classroom can be written as:

$$\mathcal{S} = \{\text{learned, unlearned}\} = \{0, 1\}$$

$\mathcal{C} = \{(1, 1), (1, 2), \dots, (1, L), (2, 1), (2, 2), \dots, (2, L), \dots, (L, L)\}$  where  $L$  is the length of the square classroom.

$\mathcal{L} = f(c) \leftarrow [L_c = \{(i + \delta i, j + \delta j) \mid (\delta i \wedge \delta j), \delta i, \delta j \in \{-1, 0, 1\}\}]$  as a mapping for outer-totalistic Moore neighborhood of radius  $r = 1$  with a fixed boundary condition.

$\mathcal{N} = \{00000000, 00000001, \dots, 11111111\}$  such that the representation of the neighborhood state  $N_c \in \mathcal{N}$  is equivalent to  $N_c = \{s_{i+\delta i, j+\delta j} \mid \delta i, \delta j \in \{-1, 0, 1\}\}$ .

$\mathcal{R}$  = the probabilistic rule defined by equation 2.2.

The numerical procedure is outlined in Figure 2.1. Each simulation for the traditional model starts with all students unlearned. The simulation is considered finished once all the students have learned.

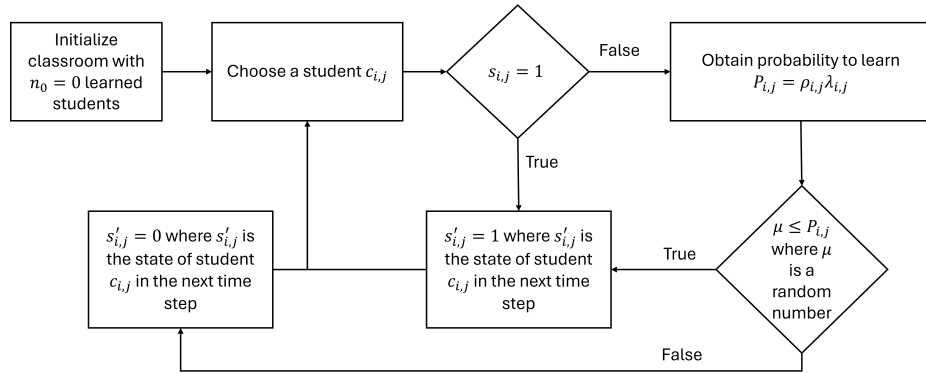


Figure 2.1: Numerical process for simulation of 2D BPCA for traditional set-ups.

(figure) shows an example of a classroom's evolution over time in the traditional set up. The sample classroom is set with  $L = 64$ ,  $\lambda_0 = 1$ , and  $\rho_0 = 0.5$ .

### 2.2.2 Peer instruction (PI)

To model the learning process in a PI set up, we set the probability for the student to learn in each time  $P_{ij}$  to be dependent on three factors. First (1), their learning rate  $\lambda_{i,j}$ . Secondly (2), the positional learning factor  $\rho_{i+\delta i, j+\delta j}$  which describes how likely it is to learn from the neighbor  $c_{i+\delta i, j+\delta j}$  based solely on their relative position with respect to  $c_{i,j}$ . Lastly (3), the aptitude level of the neighbor  $s_{i+\delta i, j+\delta j}$  which dictates

whether student  $c_{i,j}$  can learn from them. The probability for a student to learn in each time step is then determined by the following equation:

$$P_{ij} = 1 - \prod_{\delta i, \delta j} [1 - (\lambda_{ij})(\rho_{i+\delta i, j+\delta j})(s_{i+\delta i, j+\delta j})] \quad (2.3)$$

where

$P_{i,j} \in [0, 1]$  is the probability of student  $c_{i,j}$  to learn in each time step,

$\lambda_{i,j} = 1$  is the learning rate of student  $c_{i,j}$

$\rho_{i+\delta i, j+\delta j} \in [0, 1]$  is the probability of  $c_{i,j}$  to learn from their neighbors in seats  $\{c_{i+\delta i, j+\delta j} \forall \delta i, \delta j \in \{-1, 0, 1\}\}$  solely based from their relative positions with each other, and

$s_{i+\delta i, j+\delta j} = \{\text{unlearned, learned}\} = \{0, 1\}$  are the neighbors' aptitude level.

The derivation of Equation 2.3 is shown in Appendix A.1.

The numerical procedure is outlined in Figure 2.2. Each simulation starts the classroom with four learned students  $n_0 = 4$  placed in different seats in the classroom. The simulation is considered finished once all the students have learned.

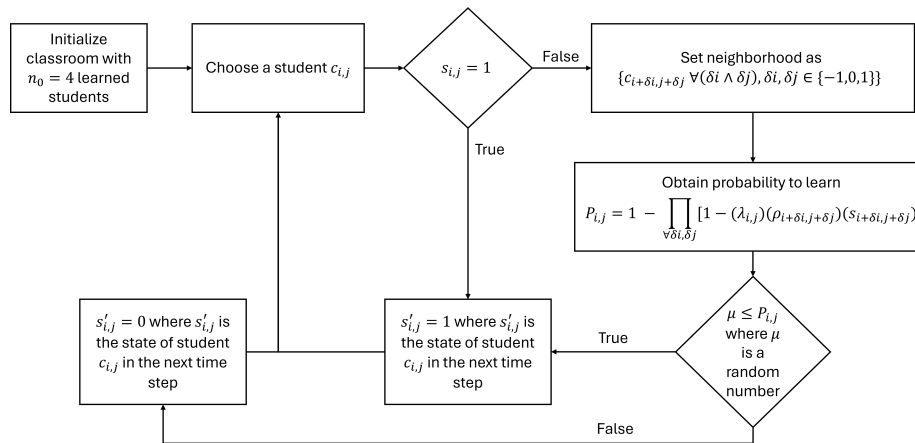


Figure 2.2: Numerical process for simulation of 2D BPCA for PI set-ups.

The seating arrangement (SA) were chosen from a previous study that shows that the SA can affect the learning process [5]. These SA's are namely: inner corner, outer corner, center, and random. The different SA's are shown in Figure 2.3.

Figure 2.4 shows an example of classroom's evolution over time. The sample classroom is set with  $L = 64$ ,  $\lambda_0 = 1$ , and  $\rho_0 = 0.5$  with the inner corner SA.

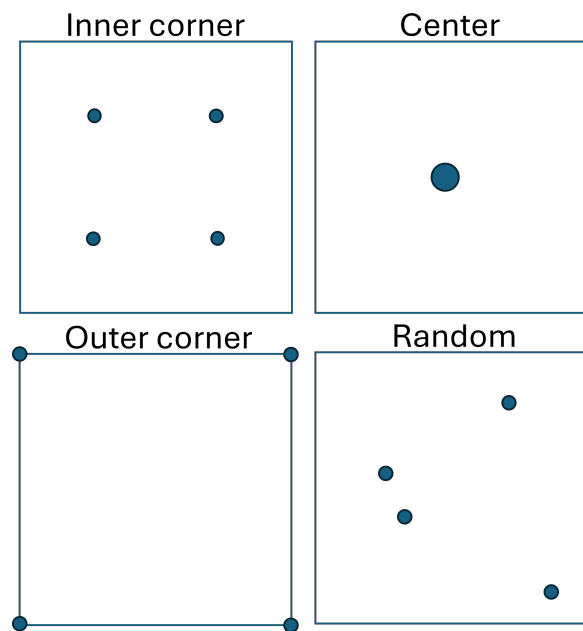


Figure 2.3: Peer instruction seating arrangements. Circles denote high aptitude students. The inner corner SA places high aptitude students halfway between the center and the corner of the classroom. The outer corner SA places high aptitude students at the corner of the classroom. The center SA places high aptitude students in the center of the classroom. The random SA places high aptitude students randomly throughout the classroom.

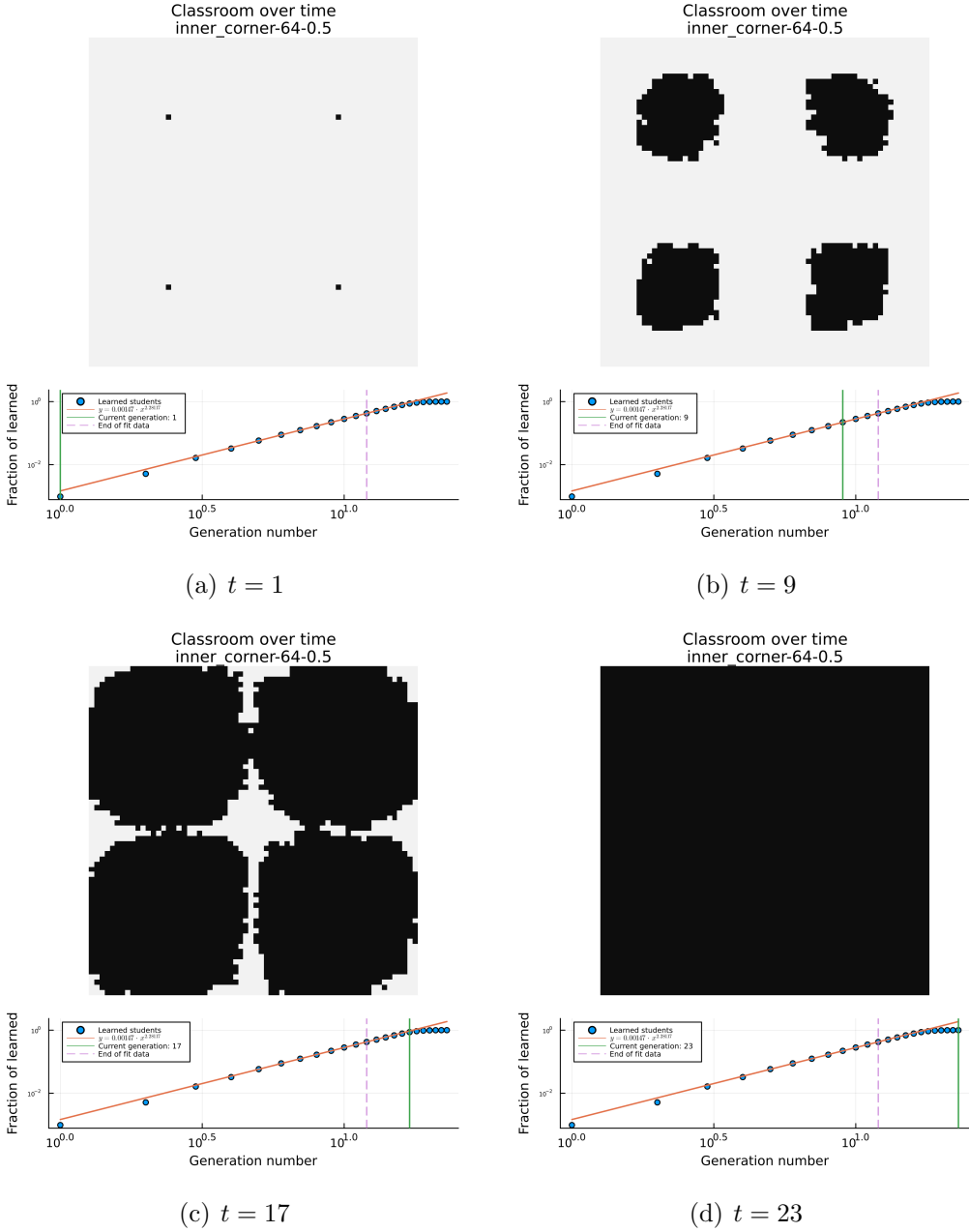


Figure 2.4: Sample classroom evolution for  $L = 64$ ,  $\lambda_0 = 1$ , and  $\rho_0 = 0.5$  with the inner corner SA. Black squares represent learned students while white squares represent unlearned students. The accompanying graphs show the fraction of learned students as a function of time. The blue circle represents the data points while the orange line shows the power law fit. The broken pink line shows where we truncate the data for fitting the power law and the green line shows the current time step in the plot.

## 2.3 Results: Homogenous PI vs Traditional

In this chapter, we only consider the case where all students have the same learning rate  $\lambda_{i,j} = \lambda_0 = 1$  and an isotropic positional learning factor  $\rho_{i,j} = \rho_0 \forall (\delta i \wedge \delta j), \delta i, \delta j \in \{-1, 0, 1\}$ . From the simulations, we compared both the average number time steps  $\langle t_{max} \rangle$  it takes for all the students in the classroom to learn and the average learning rate  $\langle m \rangle$  across different configurations over 5 independent runs. The class learning rate  $m$  for each trial was obtained by using a Levenberg-Marquardt algorithm to fit a power law ( $y = ax^m$ ) to the fraction of learned students as a function of the generation number. We only considered the first 50% of the data for the PI model and the first 25% of the data for the traditional model. This truncation was done so that we only fit the part of the data before the finite size effect starts to affect the simulation.

### 2.3.1 Time to learn $t_{max}$ vs positional learning factor $\rho_0$

The data in Figure 2.5 shows that the time to learn  $t_{max}$  decreases with increasing positional learning factor  $\rho_0$  for all classroom sizes for both traditional models and PI models. Among PI models, the inner corner SA has the lowest  $t_{max}$  for all classroom sizes. The outer corner and center SAs performed similarly, while the random SA has the highest  $t_{max}$ . The traditional model performs situationally better than even the inner corner PI model, something we will investigate in Section 2.3.3.

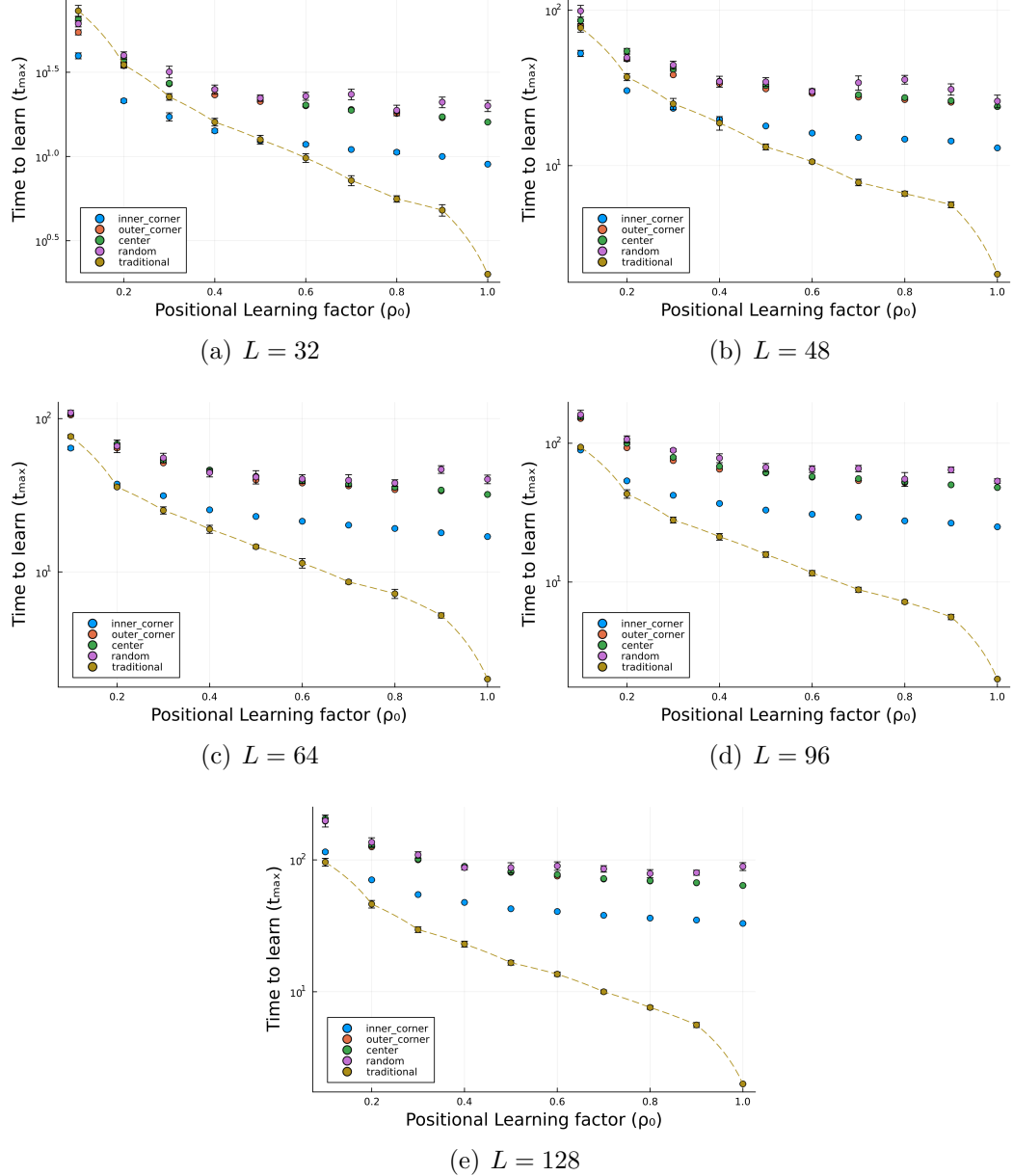


Figure 2.5: Time to learn  $t_{max}$  as a function of positional learning factor  $\rho_0$  for different classroom sizes  $L \in \{32, 48, 64, 96, 128\}$ . Lower time to learn  $t_{max}$  indicate better performance.

### 2.3.2 Class learning rate $m$ vs positional learning factor $\rho_0$

The data in Figure 2.6 shows that the class learning rate  $m$  does not generally change for different positional learning factors  $\rho_0$  when comparing against similar SAs for the PI model. The traditional model, however, shows a increase in class learning rate  $m$  with increasing  $\rho_0$  for all classroom sizes. Similar to the findings in section 2.3.1, the inner corner SA has the highest learning rate  $m$  for all classroom sizes. The outer corner and center SAs performed similarly, while the random SA has the lowest class learning rate  $m$ . We still find that the traditional model performs situationally better than even the inner corner PI model.

The sudden decrease in class learning rate  $m$  for the traditional model at  $\rho_0 = 1.0$  is due to the improper truncation and fitting of the data. In the traditional model where  $\rho_0 = 1.0$ , all the students will transition from unlearned to learned in one time step, so fitting the power law to the first 25% of the data would yield a class learning rate  $m$  that does not represent the results of the simulations well.

The results in this section show that the traditional model performs better than the PI model in terms of class learning rate  $m$  for all classroom sizes at low  $\rho_0$ . This is in contrast to the results in section 2.3.1 where the PI model performed better only in small classrooms with low positional learning factor  $\rho_0$ . This discrepancy is likely due to the different metrics used to evaluate the performance of the models. The class learning rate  $m$  is a measure of how quickly the students learn, while the time to learn  $t_{max}$  is a measure of how long it takes for all the students to learn. In cases where the classroom is large and positional learning factor  $\rho_0$  is small, the traditional model is able to teach all the students in a shorter amount of time despite the PI model being able to teach the students more effectively. *This could be what other researchers find when they claim that PI is a more effective method without accounting for the classroom room size or the students' learning rates. citation needed*

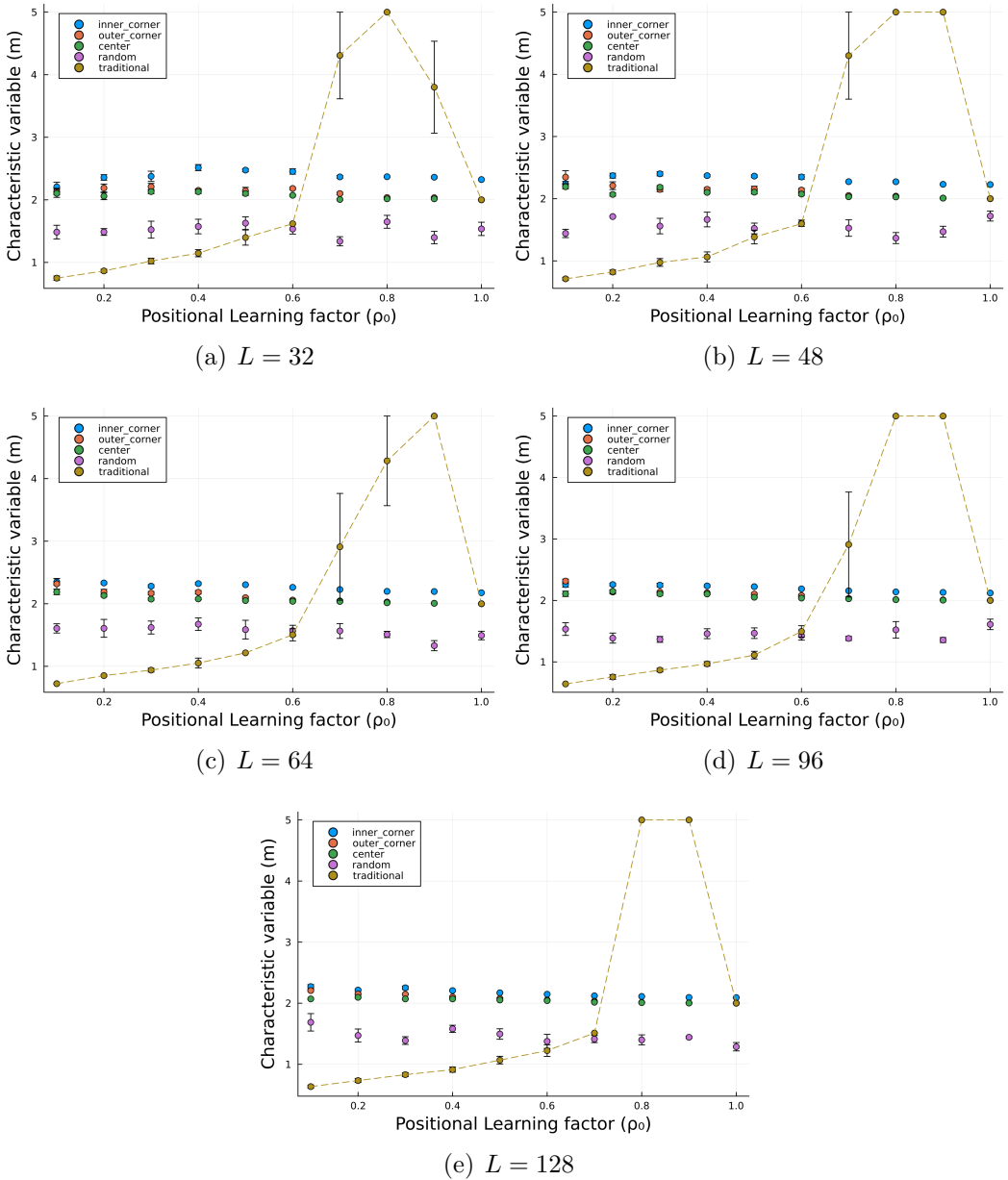


Figure 2.6: Class learning rate  $m$  as a function of positional learning factor  $\rho_0$  for different classroom sizes  $L \in \{32, 48, 64, 96, 128\}$ . Higher class learning rate  $m$  values indicate better performance.

### 2.3.3 Time to learn $t_{max}$ vs class size $N$

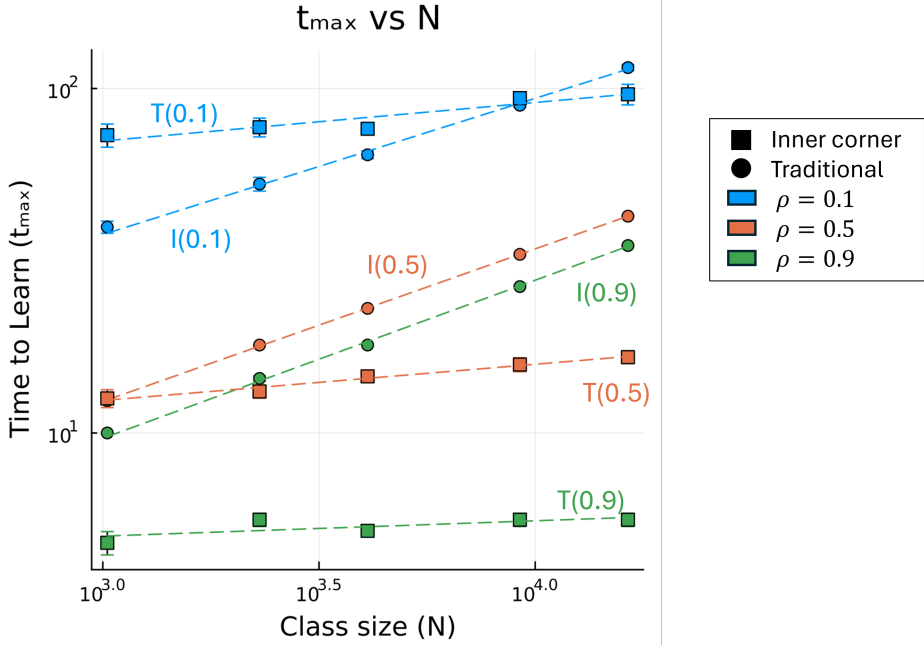


Figure 2.7: Time to learn  $t_{max}$  as a function of class size  $N$  for PI and traditional models. Circles and squares denote data points for the PI model (inner corner SA) and traditional learning model, respectively. The dash lines are the corresponding power law fit of the form  $t_{max} = a \cdot N^b$  using  $\rho \in \{0.1, 0.5, 0.9\}$ . The fitted parameters are shown in the table with an average of  $\langle b \rangle = 0.4532 \pm 0.019$  for the inner corner and  $\langle b \rangle = 0.087 \pm 0.021$  for the traditional model. Lower time to learn  $t_{max}$  indicate better performance.

	Inner corner		Traditional	
	$a$	$b$	$a$	$b$
$\lambda = 0.1$	2.4515	0.3955	32.4884	0.1119
$\lambda = 0.5$	0.5795	0.4428	6.0079	0.1052
$\lambda = 0.9$	0.4055	0.4589	3.6914	0.0445

Table 2.1: Power law fit parameters  $a$  and  $b$  for  $t_{max}$  vs  $N$ , where  $t_{max} = a \cdot N^b$

When we analyze the dependence of the time to learn  $t_{max}$  on the class size  $N$ , we find that the trend for both models follow the power law  $t_{max} = a \cdot N^b$ . In Figure 2.7 we observe break-even points where the traditional model becomes more efficient than the PI model. These points happen at lower class sizes and lower  $\rho$  values. We also find two major groups of power laws based on their  $b$  values, as summarized in Table 2.1. The first group has an average  $b$  value of  $\langle b \rangle = 0.4532 \pm 0.019$  for the inner corner SA, while the second group has an average  $b$  value of  $\langle b \rangle = 0.087 \pm 0.021$  for

the traditional model. The inner corner SA has higher  $b$  values than the traditional model, indicating that the traditional model is less affected by class size  $N$  and so is more scalable than the PI model.

## 2.4 Discussion/conclusions?

In this chapter, we have shown that between different seating arrangements for the PI model, the inner corner SA is the most efficient in terms of time to learn  $t_{max}$  and class learning rate  $m$ . The outer corner and center SAs performed similarly worse than the inner corner SA, while the random SA performed the worst. This is different from what existing literature has shown, where the outer corner SA is the most efficient [5]. This is likely because of the simplifications made in our model. Our model does not incorporate factors such as the similarity effect mentioned in previous studies [5, 6]. This effect is the phenomenon where in students of similar aptitude levels tend to learn better when seated together and are able to learn from each other regardless their actual aptitude. Our model also does not consider anisotropic positional learning factors  $\rho_{i,j}$ , where the probability of learning from a neighbor varies with the neighbors' relative positions. Besides being binary, which introduces granularity, our model also does not consider that not all students are equally receptive to peer instruction or have the same learning rate. Introducing these factors, some of which we will explore in the next chapters, may make our model reflect reality better and provide us with better understanding of the learning dynamics in the classroom.

The nature of our model lends itself to be heavily influenced by geometric factors. The most impactful factor in this case is then the distance  $d_{max}$  of any student to a high aptitude or learned student as shown in figure 2.8. The inner corner SA minimizes  $d_{max}$ , which is why it is the most efficient. The outer corner and center SAs have equal  $d_{max}$  higher than the inner corner SA, which explains why they performed very similarly albeit worse than the inner corner SA.

Our analysis on the dependence of  $t_{max}$  on  $N$  gives us an explanation on why the traditional model performed better than the PI model in most cases. With lower  $b$ -values, the traditional model is less affected by class size than the PI models are. Because of this, the traditional model performed better in cases with larger classrooms.

With regards to the performance of PI methods with traditional teaching methods,

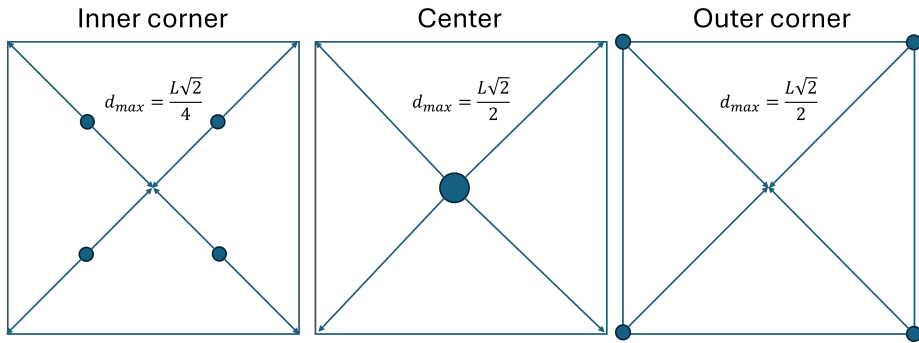


Figure 2.8: Distance  $d_{max}$  of any student to a high aptitude or learned student for different seating arrangements.

we found that classrooms with higher  $\rho_0$  values performed better in PI models, while classrooms with lower  $\rho_0$  values performed better in traditional models. A previous similar study [5] found that classes with lower aptitude levels were the ones who benefited the most from the PI methods. Although we cannot directly conclude this from our model, we were able to show that students with a lower probability of learning or students who learn slower, can benefit as much from PI as in traditional set ups. This reinforces other studies' findings [2] that show that PI methods can be effective even regardless of the students' actual aptitude levels.

# Chapter 3

## Heterogeneous Learning Rates

To introduce learning rate heterogeneity in the classroom, we revisit equation 2.3.

$$P_{ij} = 1 - \prod_{\forall \delta i, \delta j} [1 - (\lambda_{ij})(\rho_{i+\delta i, j+\delta j})(s_{i+\delta i, j+\delta j})] \quad (2.3 \text{ revised})$$

We can adjust the parameter  $\lambda_{ij}$  to introduce differences in each student's learning rate. We set a student's learning rate as  $\lambda_{ij} = \lambda_0 \pm \delta\lambda$  where  $\delta\lambda \in \{0.0, 0.1, 0.2, 0.3, 0.4\}$  and  $\lambda_0 = 0.5$ . Each student has an equal chance of having a learning rate that is either faster ( $\lambda_0 + \delta\lambda$ ) or slower ( $\lambda_0 - \delta\lambda$ ) than the average learning rate  $\lambda_0$ .

$\lambda_{i,j} \in [0, 1]$  is the learning rate of student  $c_{i,j}$  with values  $\lambda_{i,j} = \{\lambda_0 \pm \delta\lambda\}$  where  $\lambda_0 = 0.5$  and  $\delta\lambda = \{0.1, 0.2, 0.3, 0.4\}$ ,

### 3.1 Effects on classroom evolution

#### 3.1.1 Peer Instruction Models

As shown in the figures in this section, we notice values of  $\rho_0$  is still the most important factor in determining class performance. However, irregularities in the shapes of the "wave of learning" become more pronounced for lower values of  $\rho_0$  and high values of  $\delta\lambda$  as shown in figure 3.1. These irregularities are also more pronounced at the start of the classroom and fades over time. For high values of  $\rho_0$ , high values of  $\delta\lambda$  leads to the irregularity in the "wave of learning" to persist longer than those with lower values of  $\delta\lambda$ . The irregularities in both the shape of the "wave of learning" and the deviation from the power law are less pronounced for higher values of  $\rho_0$ , regardless of the value of  $\delta\lambda$ , as shown in figure 3.2 and 3.3. There are some sets of parameters who deviate from the power law fit. For peer instruction, these deviations happen for

low values of  $\rho_0$ . In these cases, the class learning rate is slower than the power law fit at the start of the simulation.

### 3.1.2 Traditional Models

For the traditional model, even though the value of  $\rho_0$  is still an important factor in determining class performance, the effect of  $\delta\lambda$  is more pronounced compared to the PI model. The trend we see in the traditional model that is absent or less evident in the PI model, is that majority of the students that learn earlier in the simulations are fast learning students (Figure 3.4(a)). After this period, most of the simulation time is spent waiting for the slow learning students to learn. This behavior is more pronounced for higher values of  $\delta\lambda$  and lower values of  $\rho_0$  as shown in Figure 3.4. This could explain the deviation from the power law fit at earlier times  $t$  for the traditional model considering that the deviation shows that the class learning rate is higher than the fitted power law.

### 3.1.3 Comparing temporal learning dynamics of different classroom configurations

When varying the class size  $L$ , as in Figure 3.5(a), we see that the traditional model's performance remains generally unchanged, with only the time to learn  $t_{max}$  increasing as the class size  $L$  increases. For PI models, an increase in class size  $L$  adds a time delay to when the learning starts to speed up. Despite the added time delay, the general shape of the learning curve remains the same.

When varying the positional learning factor  $\rho_0$ , we see that idk

Figure 3.5(c) shows that an increase in heterogeneity  $\delta\lambda$  changes how fast the slope of the learning curve changes for the traditional model, while mostly not affecting PI models.

As shown in Figure 3.5(d), when comparing between the different SA's, at least for  $L = 64, \rho_0 = 0.5, \lambda = 0.5 \pm 0.2$ , the traditional model generally performs better than PI models, especially in the early time steps. Among the different SA's for the PI model, the inner corner SA still performs the best while the center and outer corner SAs perform similarly, the same conclusion we got from the homogenous case. Contrary to the results of the homoegnous classrooms, the random SA did not perform the worst, it performed better than the center and outer corner SA's.

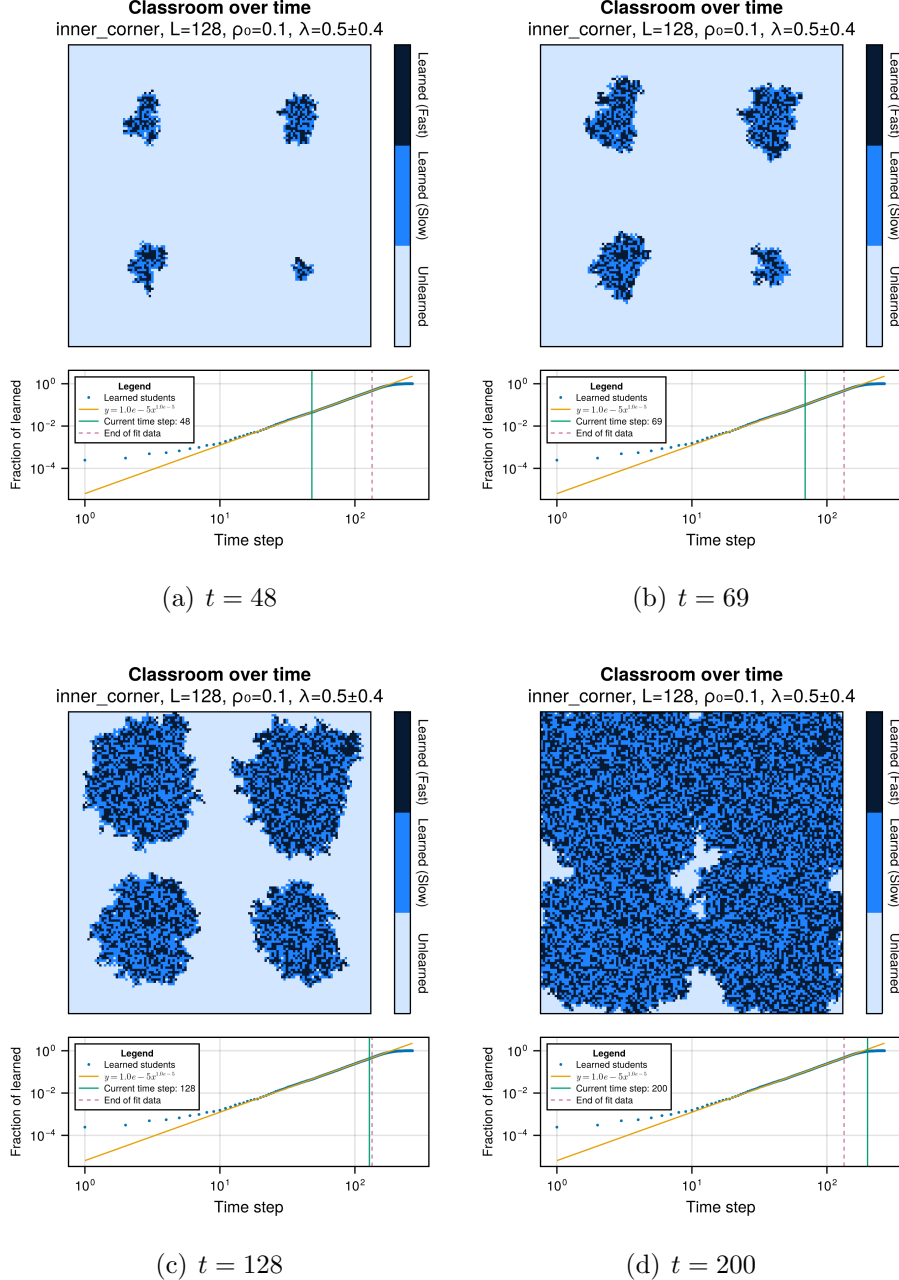


Figure 3.1: Sample classroom evolutions for the inner corner SA with  $L = 128$  at different times  $t$  for positional learning rate  $\rho_0 = 0.1$ ,  $\delta\lambda = 0.4$ . Dark blue squares represent learned students with learning rate  $\lambda = \lambda_0 + \delta\lambda$ , blue squares represent learned students with learning rate  $\lambda = \lambda_0 - \delta\lambda$ , and light squares represent unlearned students. The accompanying graph shows the fraction of learned students as a function time step. The blue dots represent data points. The yellow line shows the power law fit. The pink dashed vertical line shows where we truncate the data for fitting the power law. The green vertical line shows the current time step in the simulation.

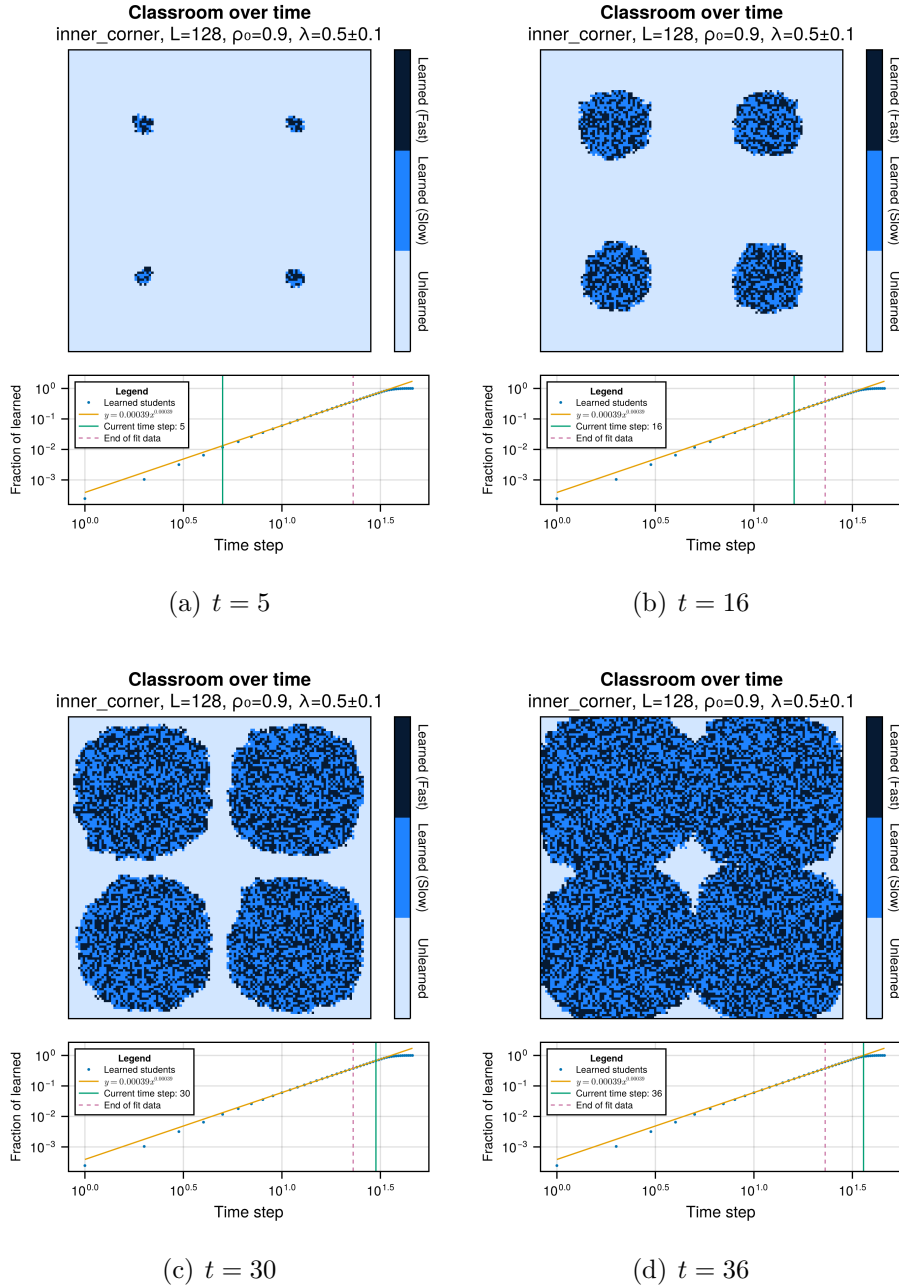


Figure 3.2: Sample classroom evolutions for the inner corner SA with  $L = 128$  at different times  $t$  for positional learning rate  $\rho_0 = 0.9$ ,  $\delta\lambda = 0.1$ . Dark blue squares represent learned students with learning rate  $\lambda = \lambda_0 + \delta\lambda$ , blue squares represent learned students with learning rate  $\lambda = \lambda_0 - \delta\lambda$ , and light squares represent unlearned students. The accompanying graph shows the fraction of learned students as a function time step. The blue dots represent data points. The yellow line shows the power law fit. The pink dashed vertical line shows where we truncate the data for fitting the power law. The green vertical line shows the current time step in the simulation.

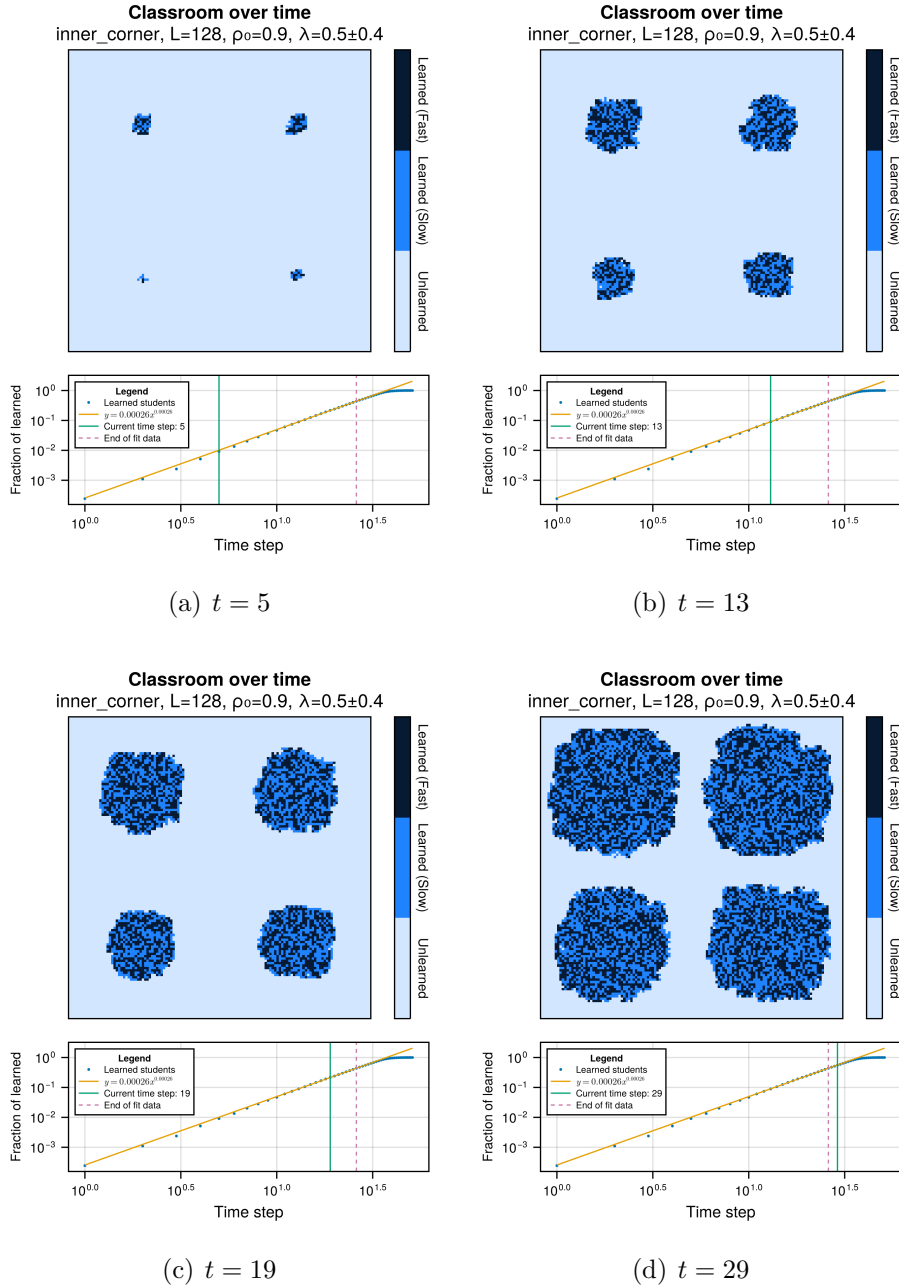


Figure 3.3: Sample classroom evolutions for the inner corner SA with  $L = 128$  at different times  $t$  for positional learning rate  $\rho_0 = 0.9$ ,  $\delta\lambda = 0.4$ . Dark blue squares represent learned students with learning rate  $\lambda = \lambda_0 + \delta\lambda$ , blue squares represent learned students with learning rate  $\lambda = \lambda_0 - \delta\lambda$ , and light squares represent unlearned students. The accompanying graph shows the fraction of learned students as a function time step. The blue dots represent data points. The yellow line shows the power law fit. The pink dashed vertical line shows where we truncate the data for fitting the power law. The green vertical line shows the current time step in the simulation.

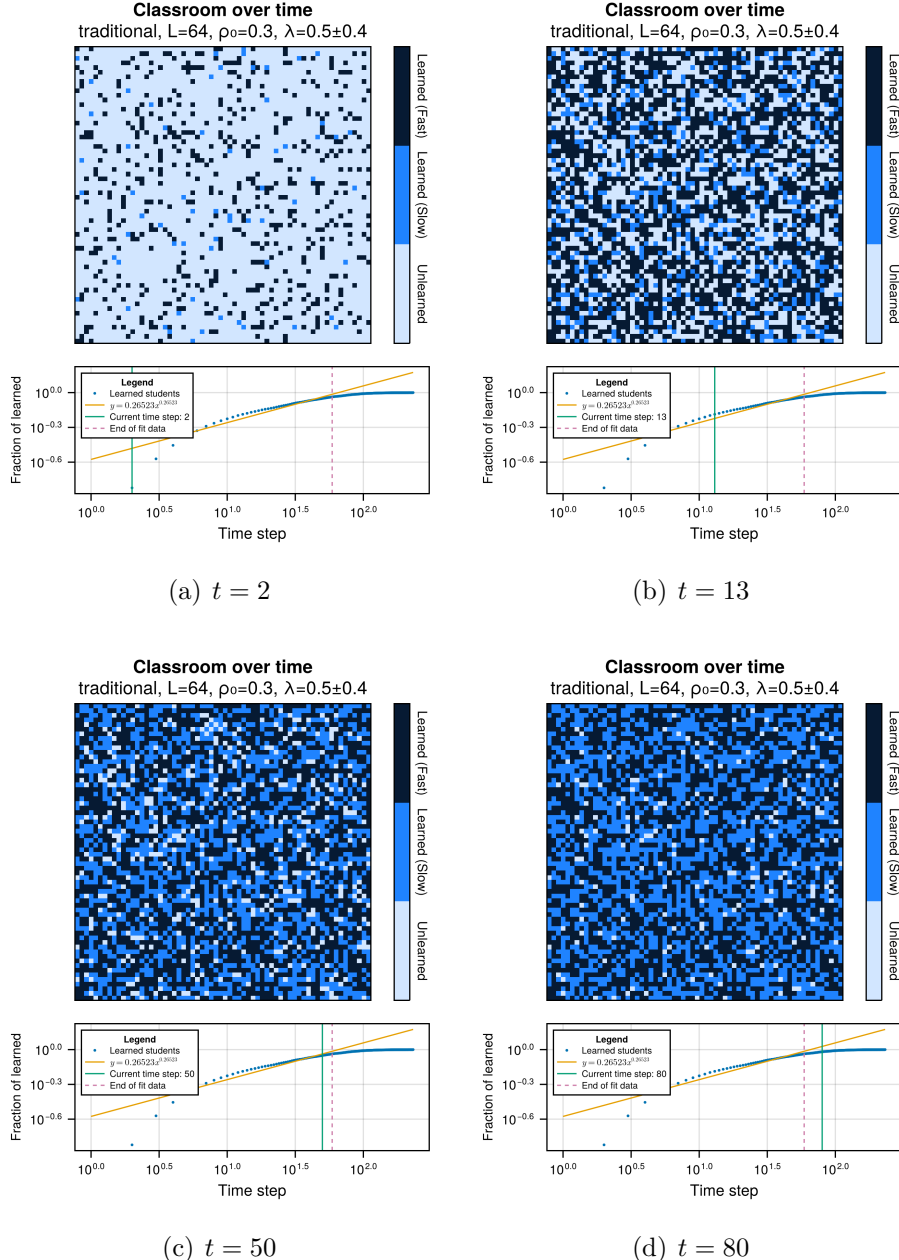


Figure 3.4: Sample classroom evolutions for the inner corner SA with  $L = 128$  at different times  $t$  for positional learning rate  $\rho_0 = 0.9$ ,  $\delta\lambda = 0.4$ . Dark blue squares represent learned students with learning rate  $\lambda = \lambda_0 + \delta\lambda$ , blue squares represent learned students with learning rate  $\lambda = \lambda_0 - \delta\lambda$ , and light squares represent unlearned students. The accompanying graph shows the fraction of learned students as a function time step. The blue dots represent data points. The yellow line shows the power law fit. The pink dashed vertical line shows where we truncate the data for fitting the power law. The green vertical line shows the current time step in the simulation.

One observation that is consistent with all the comparisons shown in Figure 3.5 is that even though the traditional model has more students learning in the early time steps, they also spend more time waiting for the last few students to learn. In contrast to this, PI models may take some time before the learning starts to speed up, but once majority of the students have learned, it does not take long until all the students to learn. This makes PI models having a shorter time to learn  $t_{max}$ , despite being outperformed by the traditional model in early time steps. This phenomenon is further investigated in the next sections where we look closer at the different factors that can affect which set up is better for a given classroom configuration.

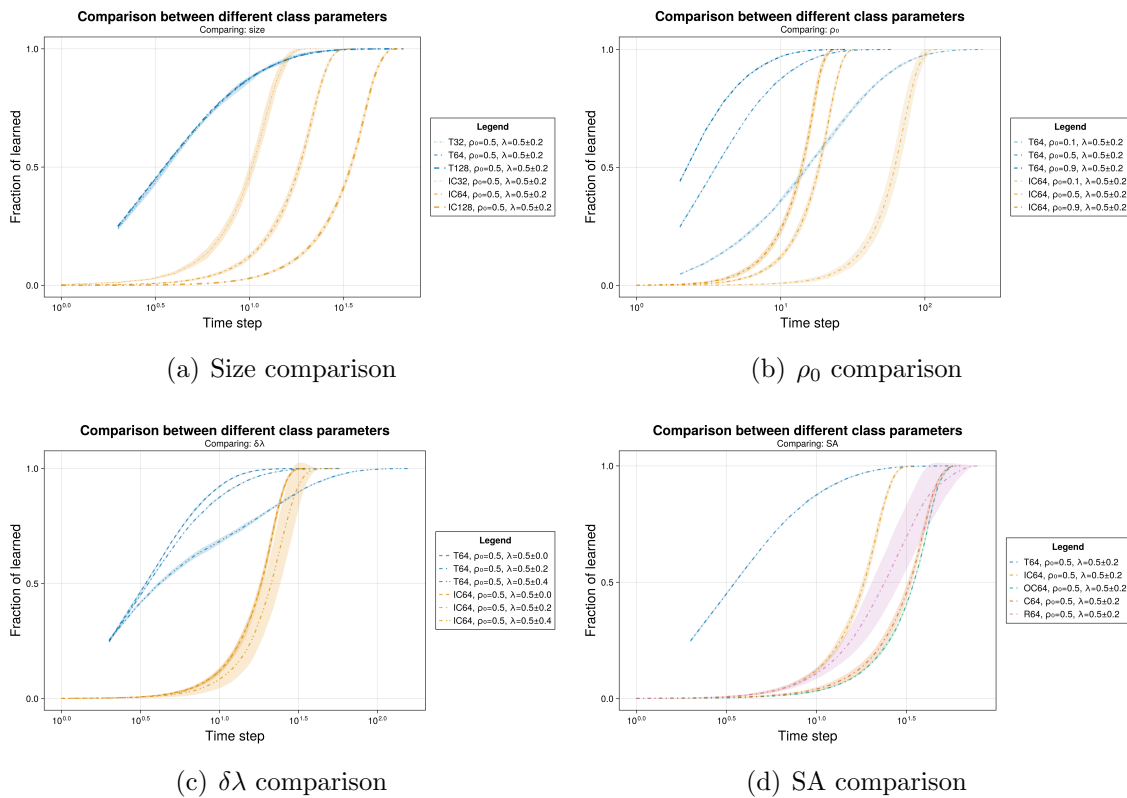


Figure 3.5: Comparison of time to learn  $t_{max}$  and fraction of learned students for different representative classroom configurations. Each SA corresponds to a different color, blue for traditional, yellow for inner corner, green for outer corner, orange for center, and pink for random. Different values  $\rho_0$  corresponds to varying alpha or transparency, where lower  $\rho_0$  values are more transparent. Different values of  $\delta\lambda$  corresponds to different line styles, where  $\delta\lambda = 0.0$  are represented by dashed lines,  $\delta\lambda = 0.2$  are represented by lines with alternating dots and dashes,  $\delta\lambda = 0.4$  are represented by two dots followed by a dash. Different classroom sizes  $L$  corresponds to different line widths, where bigger classroom sizes correspond to thicker lines. The bands around each line show the standard deviation of the data over 5 trials. Higher fraction of learned indicates better performance.

### 3.2 Class learning rate $m$ vs positional learning factor $\rho_0$

Figure 3.6 shows that class learning rate becomes inconsistent with the positional learning factor  $\rho_0$  in PI models when introducing heterogeneity. With heterogeneity, PI models no longer show trends in learning rate  $m$  as a function of positional learning factor  $\rho_0$ . The traditional model shows a similar trend in learning rate  $m$  as with time to learn  $t_{max}$  where homogenous classrooms perform better than heterogeneous classrooms. This might be explained by the spatiotemporal dynamics of traditional learning models where the fast learning students learn first and the slow learning students learn last, as discussed in section 3.1 and shown in figure 3.4.

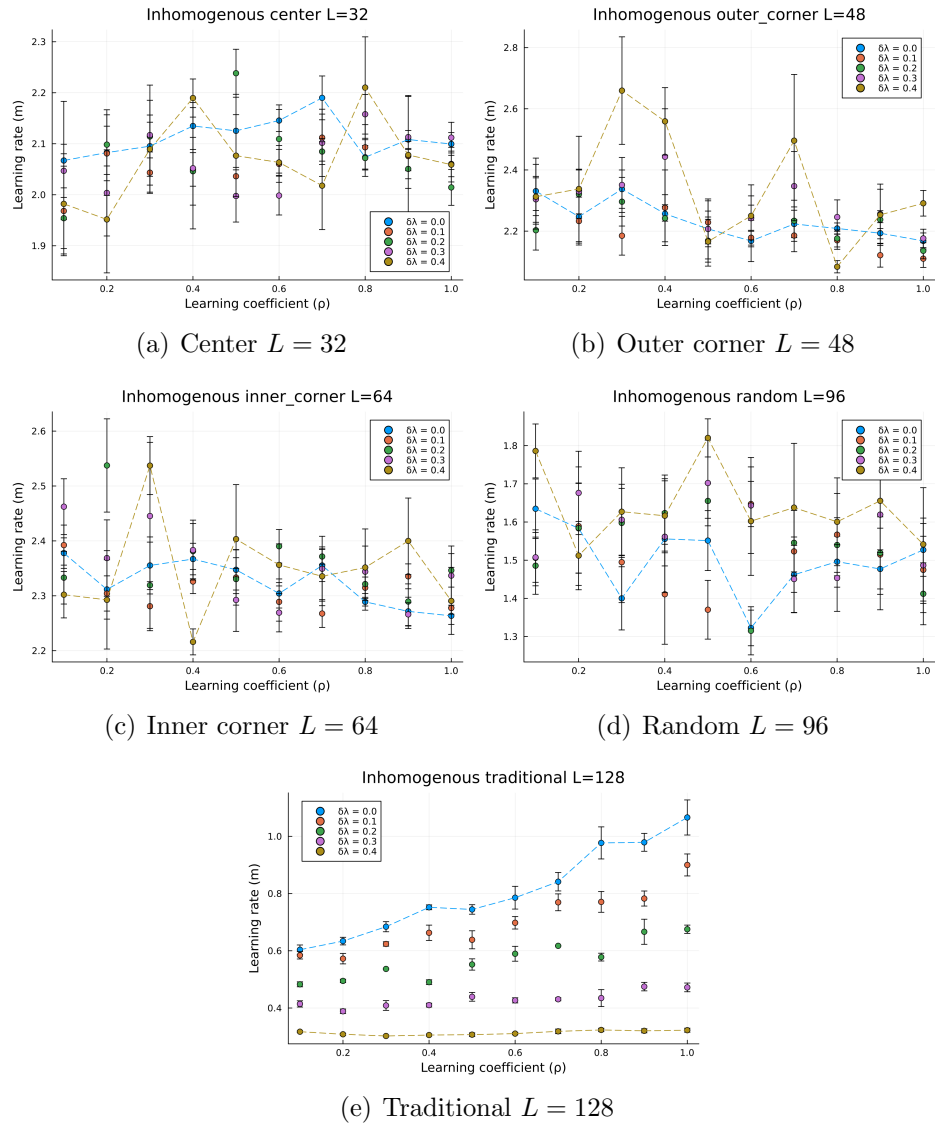


Figure 3.6: Representative plots for class learning rate  $m$  as a function of positional learning coefficient  $\rho_0$ . Each subplot represent a different SA and classroom size  $L$ . In each plot, the circles represent the data points, color represents a different value of  $\delta\lambda \in \{0.0, 0.1, 0.2, 0.3, 0.4\}$ , dashed lines connect the data points for  $\delta\lambda \in \{0.0, 0.4\}$ . Higher class learning rate  $m$  values indicate better performance.

### 3.3 Time to learn $t_{max}$ vs positional learning factor $\rho_0$

Figure 3.7 shows the time to learn  $t_{max}$  is directly affected by the level of heterogeneity  $\delta\lambda$ . This means that the heterogeneity  $\delta\lambda$  has a significant effect on the time to learn  $t_{max}$ , with lower values of  $\delta\lambda$  leading to lower time to learn  $t_{max}$  for all values of  $\rho_0$ . We also notice that the traditional model is more affected by classroom heterogeneity compared to PI models.

When aggregating the different results for each class size  $L$ , as shown in Figure 3.8, it affirms our previous findings that PI models are better for smaller classes and lower values of  $\rho_0$ . This stays consistent when comparing the performance of a similar classroom size  $L$  and heterogeneity  $\delta\lambda$  using the traditional model. However, the comparison is not as clear when comparing between different levels of heterogeneity  $\delta\lambda$ . When  $L \geq 64$ , the PI models can perform better than the traditional model depending on the heterogeneity  $\delta\lambda$ , even with the same positional learning factor  $\rho_0$ .

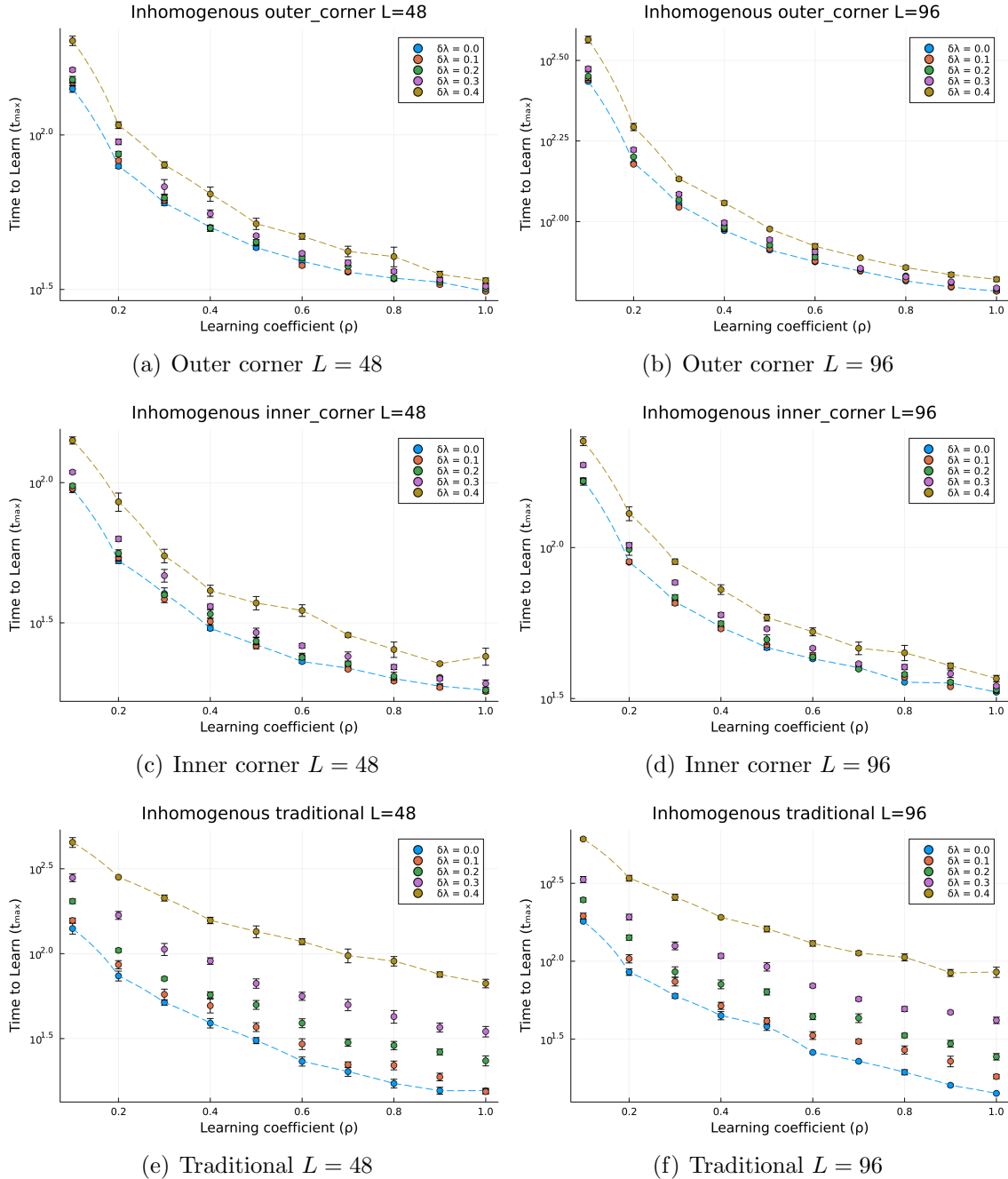


Figure 3.7: Time to learn  $t_{max}$  as a function of positional learning factor  $\rho_0$  for different representative classroom configurations and sizes with varying heterogeneity  $\delta\lambda \in \{0, 0.1, 0.2, 0.3, 0.4\}$ . Lower time to learn  $t_{max}$  indicates better performance.

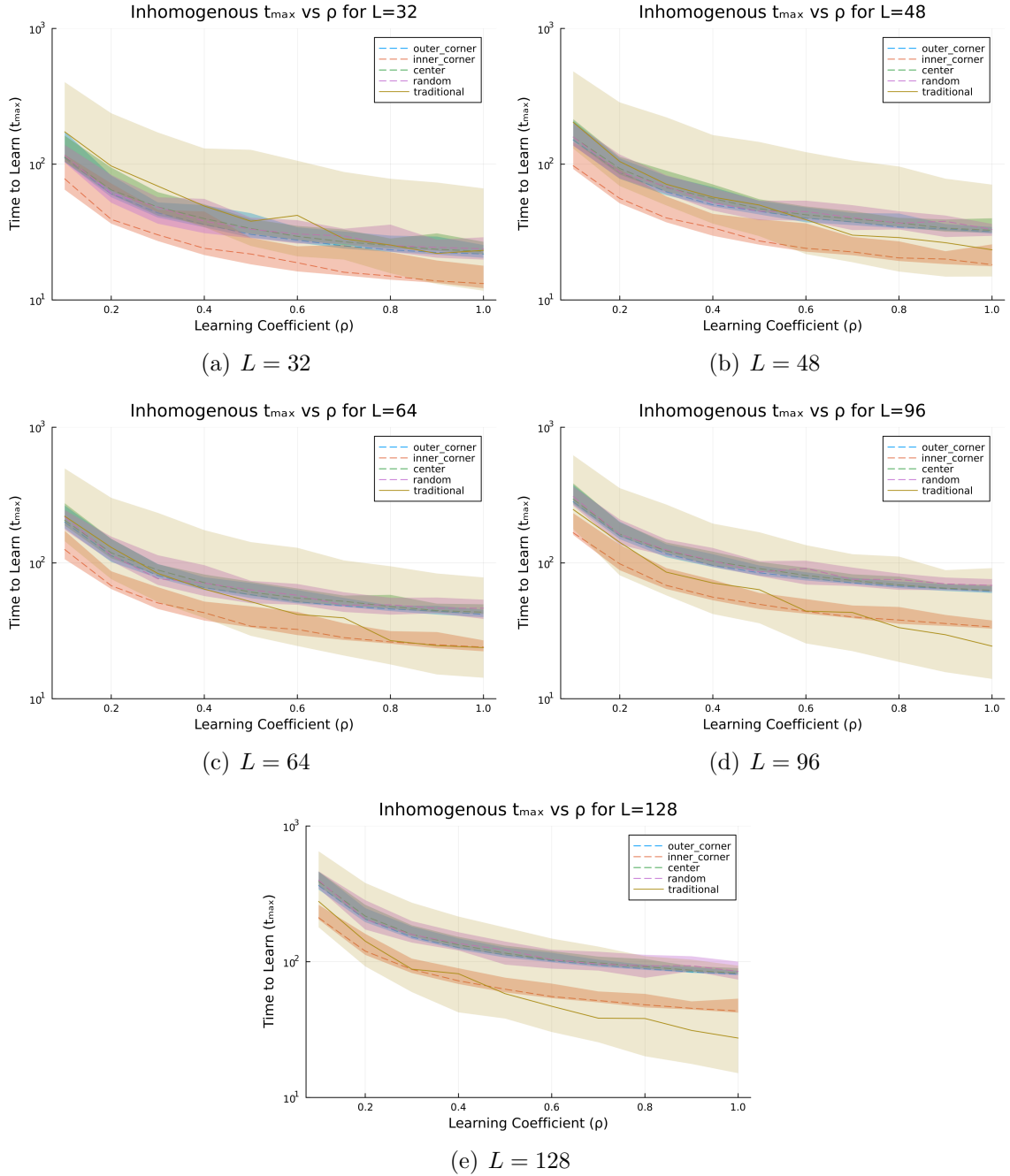


Figure 3.8: Time to learn  $t_{max}$  as a function of positional learning factor  $\rho_0$  for the heterogeneous model of all seating arrangements and classroom sizes  $L$ . Each ribbon series represent the range of values for  $t_{max}$  for a given seating arrangements with heterogeneity  $\delta\lambda = \{0.0, 0.1, 0.2, 0.3, 0.4\}$ . Lower time to learn  $t_{max}$  indicates better performance.

### 3.4 Class learning rate $m$ vs heterogeneity $\delta\lambda$

### 3.5 Time to learn $t_{max}$ vs heterogeneity $\delta\lambda$

Figure 3.9 shows that as heterogeneity  $\delta\lambda$  increases, PI methods perform better than traditional methods even when PI methods have lower positional learning factors  $\rho_0$ . For our representative  $\rho_0$  values, PI performs better than traditional methods regardless of the  $\rho_0$  value, even in a large classroom  $L = 128$ . However, in larger classrooms, the advantage in performance of PI over traditional methods is less pronounced. Furthermore, as class size increases, traditional methods tend to stay advantageous than PI methods for increasing values of heterogeneity  $\delta\lambda$ .

For example, at  $L = 32$  shown in figure 3.9(a), PI methods are better than traditional methods for all values of  $\delta\lambda$  when comparing between equal  $\rho_0$  values. However, at  $L = 128$  shown in figure 3.9(b), the traditional model performs better than the PI model for  $0 \leq \delta\lambda \leq 0.2$  when comparing between equal  $\rho_0$  values.

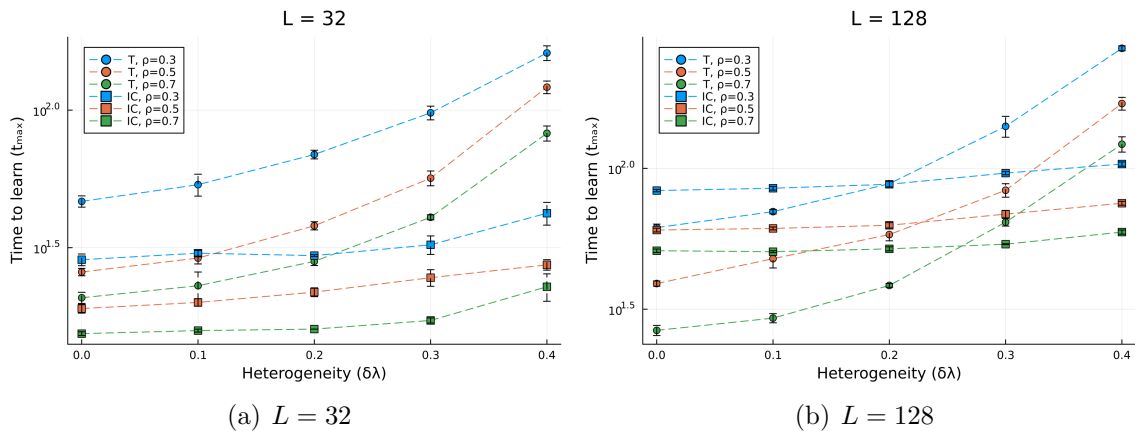


Figure 3.9: Time to learn  $t_{max}$  as a function of heterogeneity  $\delta\lambda$  for the heterogeneous models of the PI (inner corner SA) and traditional models with varying positional learning factor  $\rho_0 \in \{0.3, 0.5, 0.7\}$  and classroom sizes  $L \in \{32, 128\}$ . Each color represents a different value of  $\rho_0$ , while the circle and square symbols represent the traditional and PI models respectively. Lower time to learn  $t_{max}$  indicates better performance.

### 3.6 Discussions/Conclusions?

- PI models still better for small classrooms, traditional models better for large class sizes. Same for both homogenous and heterogeneous.

- heterogeneity can sway which set up is advantageous. Low heterogeneity favors traditional models, high heterogeneity favors PI models. Need to add plots for easier explanation.
- Traditional models are more sensitive than heterogeneity. Higher difference, less effective traditional models.
- Initial learning rate for traditional models is fast, but overall time to learn is longer than PI models. Natural consequence: trad then PI. This is what is done currently.

# Chapter 4

## Mixed Model Instuction

In this chapter, a sample for making equations and sub-equations are demonstrated.

### 4.1 Equations and sub-equations

In the following, a set of equations is shown.

$$\vec{\nabla} \cdot \vec{D} = \rho \quad (4.1a)$$

$$\vec{\nabla} \cdot \vec{B} = 0 \quad (4.1b)$$

$$\vec{\nabla} \times \vec{E} = -\partial_t \vec{B} \quad (4.1c)$$

The last one being

$$\vec{\nabla} \times \vec{H} = \vec{J} + \partial_t \vec{D} \quad (4.1d)$$

Note that text can still be placed between sub-equations within the `subequations` environment.

When using a solitary equations, you may use the usual equation syntax in L<sup>A</sup>T<sub>E</sub>X.

$$E = mc^2 \quad (4.2)$$

# **Chapter 5**

## **Conclusions**

A short sample thesis/dissertation is presented. Although not complete, it will be useful for newbies in L<sup>A</sup>T<sub>E</sub>X. Any questions? email me at the following address:  
[johnrob.bantang@gmail.com](mailto:johnrob.bantang@gmail.com).

# Appendix A

## Sample appendix

This gives an example of an appendix chapter. Note that this file has been included after the line `\appendix` in `main.tex`.

### A.1 Derivation of Equation 2.3

For any event  $e$ , the desired outcome occurs with probability  $p$  or not with probability  $q$  where

$$p + q = 1. \quad (\text{A.1a})$$

For  $n$  events, each being event  $e$ :

$$\prod_{\forall e} (p_e + q_e) = 1. \quad (\text{A.1b})$$

Expanding equation A.1b, we get

$$\prod_{\forall e} p_e + \dots + \prod_{\forall e} q_e = 1. \quad (\text{A.1c})$$

where the sum of the first  $n - 1$  terms is the probability of the desired outcome occurring at least once over  $n$  events and the last term is the probability of the desired outcome not occurring at all. Thus, we can rewrite the probability of the desired outcome occurring at least once as

$$P = 1 - \prod_{\forall e} q_e. \quad (\text{A.1d})$$

substituting equation A.1a into equation A.1d, we get

$$P = 1 - \prod_{\forall e} (1 - p_e). \quad (\text{A.1e})$$

## A.2 Equations in appendix

You don't need to worry about equations within the appendix since L<sup>A</sup>T<sub>E</sub>X automatically formats the equation numbers for you. For example,

$$c^2 = a^2 + b^2 \quad (\text{A.2})$$

becomes the Pythagorean theorem where  $c$  is the length of the longest side of any right triangle.

## A.3 Codes as appendix

Include your codes when necessary to your thesis/dissertation. To do this, you may use `verbatim` environment as follows. **WARNING:** All verbatim and `verbatiminput` environments should always be treated as a separate paragraph. When included in a text paragraph, it sometimes happen to reduce the 1.5 spacing to the usual single-spaced text.

```
#include <iostream>
using std::cout;
using std::endl;

int main( void )
{
    cout << "Hello world!" << endl;
    return 0;
}
```

The `\small` bracketed region is used to lower the font size of the entire `verbatim` text. This will save you much space and give a more aesthetical look in your manuscript.

On the other hand, when very long codes are wished to be included automatically without the tedious cut and paste procedure, you may include them using the `\verbatiminput` command as follows. You may want to include a short description of the code of course.

```
//Johnrob Y. Bantang, Natinal Institute of Physics
//Created: 03 October 2002
// Makes new C files
// usage: newC filename
//Modifications:
```

```

// >> 21 Jan 2003, Johnrob
// included the constant AUTHOR and AFFILIATION for portability

#include <stdlib.h>
#include <iostream.h>
#include <fstream.h>
#include <strstream.h>
#include <time.h>
#include <string.h>

const char *const AUTHOR= "Johnrob Y. Bantang";
const char *const AFFILIATION= "National Institute of Physics";
const char *const EXTENSION= ".cpp";

int main(int argc,char **argv){
if(argc!=2){
cout<<"usage: newC filename"<<endl;
exit(0);
}
char *fname= new char[strlen(argv[1])+5];
ostrstream out(fname,strlen(argv[1])+5);
out<<argv[1]<<EXTENSION;
time_t date=time(NULL);

ofstream file(fname,ios::nocreate,0);
//opens normal file that **already exists**;
if(file){
for(int i=1;i<5;i++)
cout<<"WARNING! file already exists!"<<endl;
cout<<endl<<"you can type"<<endl<<endl;
cout<<"\t\"head "<<fname<<"\"\n";
cout<<"in command line to *view version*"<<endl<<endl;
cout<<"please enter 1 to OVERWRITE this file"<<endl;
cout<<"type anything to cancel"<<endl;
for(int i=1;i<5;i++)
cout<<"WARNING! file already exists!"<<endl;
int n;
cin>>n;
if(n!=1){
cout<<"\n*no* file is created... exiting..."<<endl<<endl;
exit(0);
}
file.close();
file.open(fname);
if(!file)
cout<<"**cannot create new file!!**"<<endl;
cout<<"OLD FILE: "<<fname<<" *overwritten!*"<<endl;
}
if(!file){

```

```

file.open(fname);
if(!file){
cout<<"**cannot create new file!!**"<<endl;
exit(0);
}
cout<<endl<<"NEW FILE created: "<<fname<<endl<<endl;

cout<<"\tcreating contents for the new C++ file: "<<endl<<endl;
//creating headers...
file<<//filename: \""<<fname<<"\\"<<endl;
file<<//<<AUTHOR<<, " <<AFFILIATION<<endl;
file<<//Created: "<<asctime( localtime(&date) );
//writes the time and date today; endl already in asctime();
file<<//<<endl;
file<<//Comments:<<endl;
file<<// >>"<<endl;
file<<//<<endl;
file<<//This file is generated using the \"newC generator\"..."<<endl;
file<<//Modifications:<<endl;
file<<// >>"<<endl<<endl;
file<<#include <iostream.h>"<<endl;
file<<#include <math.h>"<<endl<<endl;
//starting the main body...
file<<"int main(int argc,char **argv){"<<endl;
file<<//\tif(argc!= ...){"<<endl;
file<<//\tcout<<"usage: "<<argv[1]<<.exe ... \"<<endl;"<<endl;
file<<//\texit(1);<<endl;
file<<//\t}"<<endl;
file<<"\t//write the main body here"<<endl;
file<<"return(0);"<<endl<<"}"<<endl;

delete fname;
file.close();
cout<<endl<<"\tCREATION SUCCESSFUL!"<<endl<<endl;
return 0;
}

```

This time, you may just include your recent codes by just copy-paste-ing the codes (as long they are clean!) into the directory `codes/` in the directory where this file is saved.

# Bibliography

- [1] M Arciaga, M Pastor, R Batac, J Bantang, and C Monterola. Experimental observation and an empirical model of enhanced heap stability resulting from the mixing of granular materials. *Journal of Statistical Mechanics: Theory and Experiment*, 2009(07):P07040, 2009.
- [2] Nathaniel Lasry, Eric Mazur, and Jessica Watkins. Peer instruction: From harvard to the two-year college. *American journal of Physics*, 76(11):1066–1069, 2008.
- [3] Pierre-Yves Louis and Francesca R Nardi. *Probabilistic Cellular Automata: Theory, Applications and Future Perspectives*, volume 27. Springer, 2018.
- [4] Hideo Nitta. A mathematical model of peer instruction and its applications. *Upgrading Physics Education to Meet the Needs of Society*, pages 87–98, 2019.
- [5] RM Roxas, SL Carreon-Monterola, and C Monterola. Seating arrangement, group composition and competition-driven interaction: Effects on students' performance in physics. In *AIP Conference Proceedings*, volume 1263, pages 155–158. American Institute of Physics, 2010.
- [6] Michelle K Smith, William B Wood, Wendy K Adams, Carl Wieman, Jennifer K Knight, Nancy Guild, and Tin Tin Su. Why peer discussion improves student performance on in-class concept questions. *Science*, 323(5910):122–124, 2009.